



OPEN

Ultra-High Performance,
High-Temperature Superconducting
Wires via Cost-effective, Scalable,
Co-evaporation Process

SUBJECT AREAS:

SUPERCONDUCTING
PROPERTIES AND
MATERIALSELECTRONIC PROPERTIES AND
MATERIALSReceived
11 November 2013Accepted
31 March 2014Published
22 April 2014

Correspondence and
requests for materials
should be addressed to
S.O. (ssoh@keri.re.kr)
or A.G. (goyala@ornl.
gov)

Ho-Sup Kim¹, Sang-Soo Oh¹, Hong-Soo Ha¹, Dojun Youm², Seung-Hyun Moon³, Jung Ho Kim⁴,
Shi Xue Dou⁴, Yoon-Uk Heo⁵, Sung-Hun Wee⁶ & Amit Goyal⁶

¹Korea Electrotechnology Research Institute, Changwon, Gyeongnam 641-120, Korea, ²Korea Advanced Institute of Science & Technology, Daejeon, Korea, ³SuNAM Co. Ltd., Anseong-si, Gyeonggi-do 456-812, Korea, ⁴University of Wollongong, North Wollongong, NSW 2500, Australia, ⁵Pohang University of Science and Technology, Pohang 790-784, Korea, ⁶Oak Ridge National Laboratory, Oak Ridge, TN 37831, USA.

Long-length, high-temperature superconducting (HTS) wires capable of carrying high critical current, I_c , are required for a wide range of applications. Here, we report extremely high performance HTS wires based on 5 μm thick $\text{SmBa}_2\text{Cu}_3\text{O}_{7-\delta}$ (SmBCO) single layer films on textured metallic templates. SmBCO layer wires over 20 meters long were deposited by a cost-effective, scalable co-evaporation process using a batch-type drum in a dual chamber. All deposition parameters influencing the composition, phase, and texture of the films were optimized via a unique combinatorial method that is broadly applicable for co-evaporation of other promising complex materials containing several cations. Thick SmBCO layers deposited under optimized conditions exhibit excellent cube-on-cube epitaxy. Such excellent structural epitaxy over the entire thickness results in exceptionally high I_c performance, with average I_c over 1,000 A/cm-width for the entire 22 meter long wire and maximum I_c over 1,500 A/cm-width for a short 12 cm long tape. The I_c values reported in this work are the highest values ever reported from any lengths of cuprate-based HTS wire or conductor.

The development of the second generation high temperature superconducting (HTS) wires based on $\text{REBa}_2\text{Cu}_3\text{O}_{7-\delta}$ (REBCO, RE = rare earth elements, including Y) films has been geared towards a broad range of electric-power applications, such as underground power transmission cables, fault current limiters, motors, generators, etc. The wires are based on coated conductor technology, forming epitaxial REBCO superconducting layers on low-cost, flexible, biaxially textured metal substrates with thin oxide functional layers^{1,2}. For years, the critical current, I_c , of HTS wires has been improved significantly by minimizing high-angle grain boundaries in the films, which increases intergranular I_c , as well as by enhancing flux-pinning via the introduction of nanoscale defects into the REBCO film, which improves intragranular I_c ^{3–5}. In parallel, long-length wire fabrication has been also advanced, and kilometer-length HTS wires are commercially produced^{6,7}. Achieving high I_c , while making the price/performance metric expressed as \$/kA-m more suitable, however, is still a major technical issue from a commercial point of view. The current price/performance metric of HTS wires is too high to penetrate the markets where conventional copper wires or low temperature superconducting wires e.g. NbTi and Nb₃Sn are dominant⁸. To accelerate the use of REBCO HTS wires, their price needs to be reduced considerably by cost-effective, scalable fabrication of long-length, high I_c HTS wires.

Growth of a single layer REBCO film with high I_c over 1,000 A/cm-width has been widely recognized to be very challenging. To date, there have been only a few reports on fabrication of single layer, thick $\text{YBa}_2\text{Cu}_3\text{O}_{7-x}$ (YBCO) films having self-field I_c close to or over 1,000 A/cm-width at 75.5–77 K. Recently, I_c (77 K, self-field) of 1,018 A/cm-width was reported in 3 cm-long, 5.9 μm thick $\text{DyB}_2\text{Cu}_3\text{O}_{7-\delta}$ film grown on metallic templates prepared by electron beam deposition using two different chambers on inclined substrates⁹. For films grown on single crystal substrates, the I_c of $\sim 1,500$ A/cm at 75.5 K, self-field was reported for 9 μm thick YBCO films containing 5 mol% barium zirconium oxide (BZO) and 5 mol% Y_2O_3 . These high I_c samples were very short,

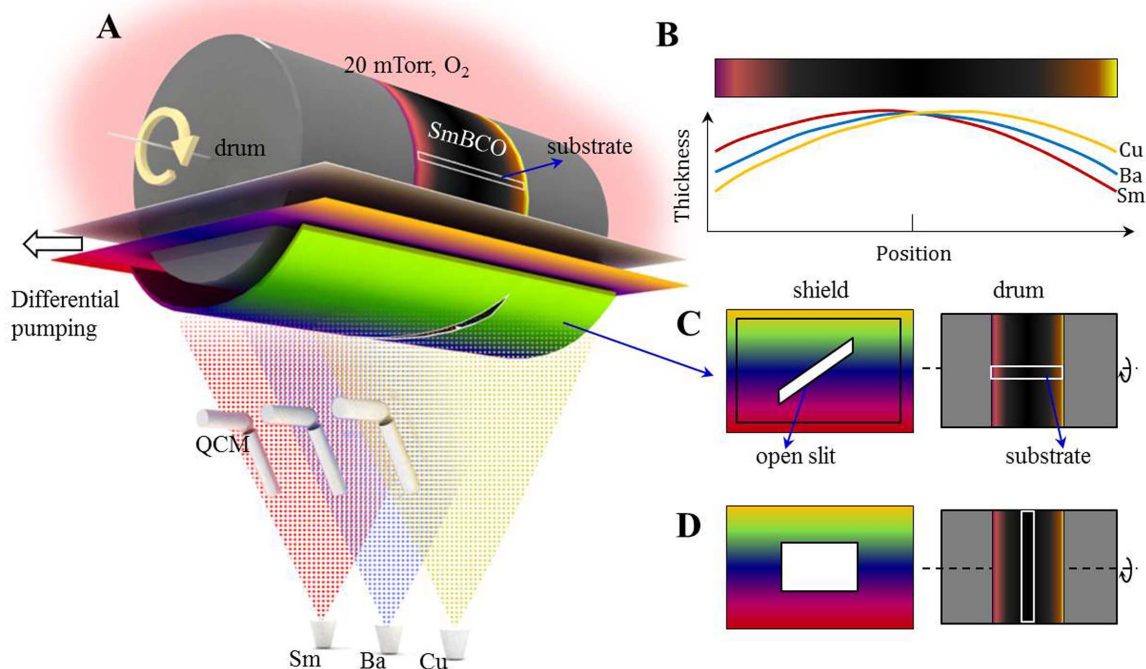


Figure 1 | Schematic outline of EDDC process with the gradient technique. (A) EDDC apparatus, consisting of an evaporation chamber, a shield plate, and a reaction chamber. Three quartz crystal microbalance (QCM) sensors are installed to detect the deposition rate of each element in the evaporation chamber. A differential pumping system is installed between the two chambers to prevent oxygen flow from the reaction chamber to the evaporation chamber. (B) Thickness distribution of each element along the substrate tape length. (C), (D) Slit geometry at the shield plate and the arrangement of substrate tape on the drum.

however, typically only a few centimeters. High I_c over 1,000 A/cm-width has never been demonstrated for HTS wires over a meter long by any HTS thin film growth technology.

To obtain a high I_c , high critical current density (J_c) should be maintained over several-micron-thick REBCO films. Generally, high J_c over 3–4 MA/cm² can be achieved in very thin film, however, J_c drops exponentially as the films get thicker¹⁰. The decay of J_c with thickness can be attributed to several factors, which include roughening of the film, loss of epitaxy or texture degradation, and reduction in the density of defects^{10,11}. We have developed a batch-type reactive co-evaporation system with a drum in a dual chamber, denoted as Evaporation using Drum in Dual Chamber (EDDC) to deposit SmBCO layers on long-length metallic templates^{12–14}. Evaporated atoms from three metal sources in high vacuum, $P(O_2) \leq \sim 1 \times 10^{-4}$ Torr, are deposited on buffered metallic templates wound on a rotating metal drum in the upper reaction chamber. Superconducting SmBCO phase forms and grows through a cyclic process of deposition-diffusion-reaction in the EDDC system.

In this process, deposition parameters can be uniformly controlled for a large chamber, so that kilometer-long HTS wires can be fabricated by merely increasing the drum size with significant modification of its basic structure. Use of inexpensive metal elements as evaporation sources can be an additional advantage, reducing the total processing cost of the wires. Several-micron-thick REBCO films can be grown easily at the same time by simply increasing the deposition time under the same deposition conditions. Considering the mass-production of REBCO wires based on Ni-textured substrate, all buffer layers can be deposited in the one EDDC system. This in-situ type EDDC approach is very promising for mass-production of REBCO wires.

We have developed a unique gradient technique to optimize the multi-variable processing parameters (such as substrate temperature, compositional ratio, and deposition rate) in a fast and reliable way. The batch-type co-evaporation process with the gradient

technique introduced in this study can be also applied to optimize deposition parameters for other functional multi-cation films such as of solar cell materials, e.g. CuInGaSe₂ (CIGS), and thermoelectric materials^{15,16}. The gradient technique allows us to control one parameter continuously along the tape length, while the other parameters remain unchanged. As shown in Figure 1, the particles of Sm, Ba, and Cu that pass through the open slit of the shield plate between the upper and lower chambers can be deposited on the substrate wound on the drum. The distribution and deposited film thickness of the atoms are affected by the shape of the open slit and the configuration of the substrate on the drum.

When using the parallelogram slit shape for the substrate arrangement shown in Figure 1(C), film with different compositions along its length is deposited in the same run. This is because the composition gradient is formed by the different amounts of each element deposited on the substrate along the tape length, as schematically shown in Figure 1(B). On the other hand, a gradient of substrate temperature along the tape length can be set up when the substrate tape is mounted perpendicular to the drum axis, as shown in Figure 1(D), and the SmBCO films are deposited after turning off half the halogen heaters inside the drum. By using the gradient technique, we can deposit a film with different compositions or several films at different deposition temperatures in the same runs and therefore, quickly optimize the overall deposition parameters.

Results

Optimization of processing parameters via the gradient technique.

In the EDDC process, J_c of REBCO films is influenced by deposition parameters such as the substrate temperature, compositional ratio, deposition rate, rotation speed of the drum, oxygen partial pressure, etc. Among the parameters, oxygen partial pressure and drum rotation speed were optimized in previous experiments. The general structure and the principles of the EDDC have been described in previous reports^{13,14}.

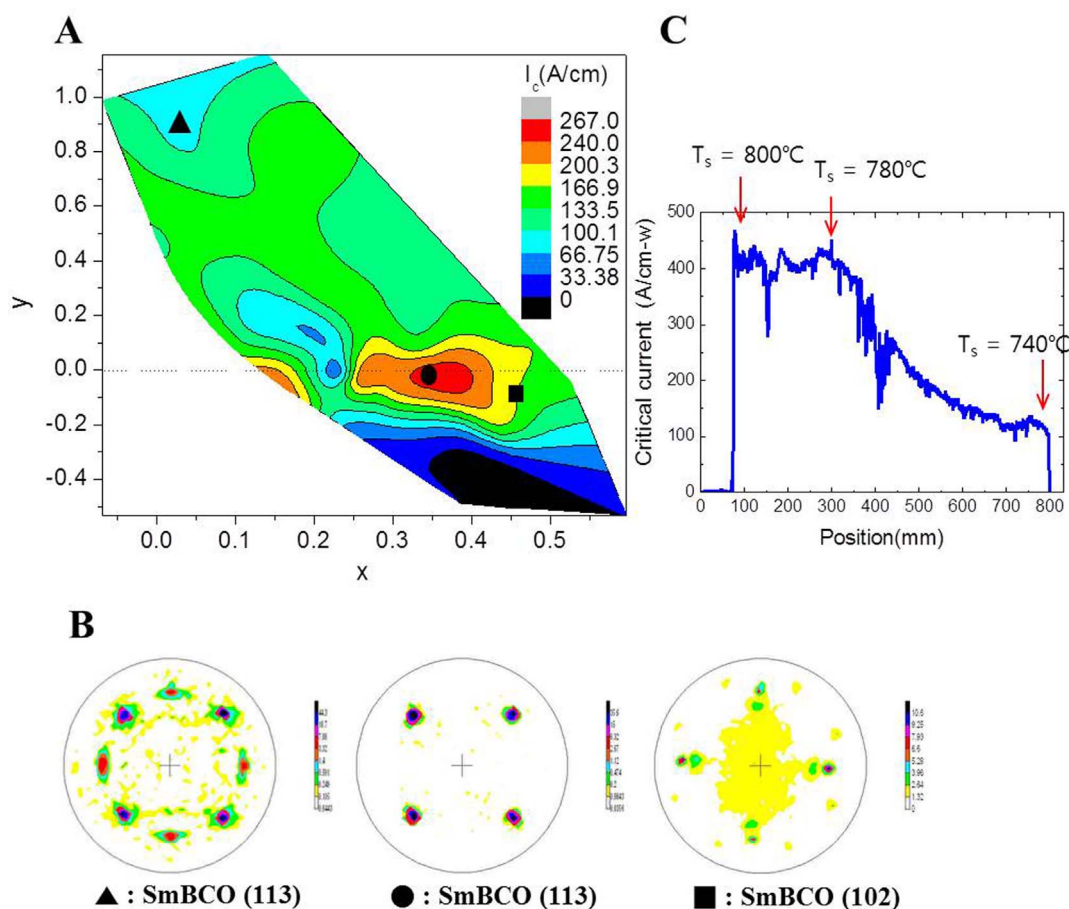


Figure 2 | The dependency of composition and substrate temperature on critical current, and X-ray pole figures of selected composition areas.

(A) Critical current versus x , y composition of SmBCO. Composition values x and y are derived from the formula of $\text{Sm}_{1+x}\text{Ba}_2\text{Cu}_3 + y\text{O}_{7-\delta}$. (B) X-ray pole figures for the positions of ▲, ●, ■ in graph (A). (C) Critical current with respect to position of the tape, where measured substrate temperatures for the deposition are indicated at selected positions.

Figure 2 summarizes the dependence of I_c for SmBCO films on film stoichiometry and deposition temperature, as obtained using the gradient technique. All samples were grown on ion-beam-assisted deposition (IBAD)-MgO templates consisting of LaMnO_3 (LMO)/MgO/ Y_2O_3 / Al_2O_3 /Hastelloy. I_c was measured continuously by a reel-to-reel Hall sensor method¹⁷. Detailed experimental procedures for the film deposition and characterization are described in section 2 in the Supplementary Information. The I_c is plotted as a function of x and y in the formula $\text{Sm}_{1+x}\text{Ba}_2\text{Cu}_3 + y\text{O}_{7-\delta}$ in Figure 2(A). The film compositions were determined by energy dispersive X-ray (EDX) analysis on the surface of the film after deposition. The results confirm that I_c is strongly dependent on the composition. The highest I_c was found in the red colored region, whose composition is slightly shifted to Sm-rich from the stoichiometric composition of Sm: Ba: Cu = 1:2:3.

X-ray diffraction (XRD) results also confirm that the samples with some excess Sm ($x \approx 0.35$), corresponding to the composition of the red colored region, have strong (00 l) orientation, without any other peaks caused by other orientations or secondary phases, and also have excellent in-plane and out-of-plane textures with cube texture over 95%. Detailed XRD results for the samples with different compositions are presented in section 2 in the Supplementary Information. Films with compositions off the red zone, as indicated by ▲ and ■ in Fig. 2(A) show low I_c performance due to their poor structural properties. XRD results reveal that the films with the composition ▲ have additional 20 peaks caused by unidentified secondary phases, and the films with the composition ■ have poor texture with an additional texture component caused by 45° oriented

SmBCO grains. The composition dependence of I_c suggests that strict control of composition is very much required for the fabrication of high I_c SmBCO films.

Figure 2(C) shows the dependence of I_c on the substrate temperature for SmBCO films. To fabricate a SmBCO film tape at different substrate temperatures, the type (D) arrangement in Figure 1 was used, and 800 nm-thick SmBCO film was deposited at the deposition rate of 7 nm/sec. The substrate temperature was measured as indicated in the graph. I_c increases as the temperature increases from 740°C and has its maximum values in the temperature range of 780 to 800°C .

After optimization of processing parameters via the gradient technique, we grew 5 μm -thick optimized SmBCO layers on IBAD-MgO templates that were over 22 meters in length. Detailed processing parameters employed for the deposition are listed in section 3 in the Supplementary Information. The composition of the thick SmBCO film was identified to be Sm: Ba: Cu = 1.33:2.00:3.00, which is within the range of the optimum composition, leading to the highest I_c in $\sim 1 \mu\text{m}$ thick SmBCO film, as shown in Fig. 2(A).

Critical current properties of SmBCO coated conductor.

Figure 3(A) shows the I_c distribution for the entire 22 meter long wire. The periodic wave pattern of I_c is caused by the deposition temperature variation along the circumference of the drum during the deposition [refer to section 4 in the Supplementary Information for further details]. Minimum and average I_c values of this tape were 633 A/cm-width and 1,157 A/cm-width, respectively. Moreover, I_c above 1,000 A/cm-width was achieved from an SmBCO tape ~ 17

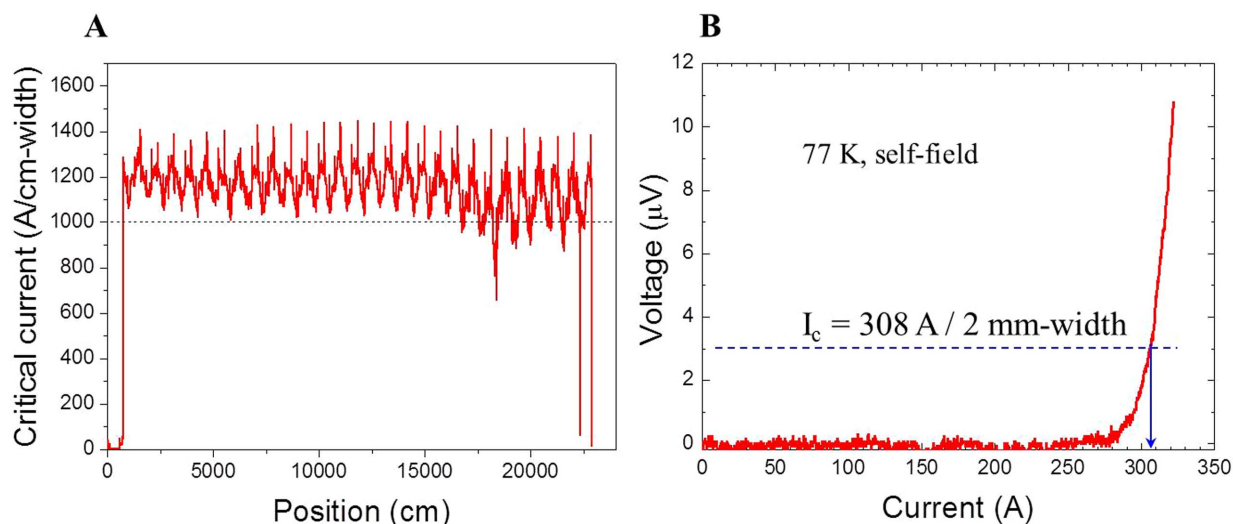


Figure 3 | Critical current distribution along the length and V-I curve. (A) I_c at 77 K, self-field of 22 m-long SmBCO tape measured using Hall sensor method. (B) Current - voltage curve for 12 cm long tape having the highest I_c . The ~ 1 cm wide sample was patterned into a ~ 2 mm wide bridge by laser-scribing, due to the limits on the maximum measuring current in the characterization system.

meters long. After I_c for the entire tape was measured continuously by a reel-to-reel Hall sensor method, the tape was cut into 12 cm-long sections to measure transport I_c values by the standard four-point probe method with a voltage criterion of 1 $\mu\text{V}/\text{cm}$.

Figure 3(B) shows the current versus voltage curve for a 12 cm long, 5 μm -thick SmBCO film, which has the highest I_c value among the 12 cm-long samples. The transport I_c (77 K, sf) was measured at 1,540 A/cm-width, which corresponds to J_c of ~ 3 MA/cm². This I_c is the highest value ever reported for any length of HTS film on either single crystal or metallic substrates. We believe that such high I_c performance is attributable to excellent structural properties that have never been observed in the REBCO thick films previously reported. XRD analysis (see section 3 in the Supplementary Information) confirms that the 5 μm thick film with the record I_c has excellent in-plane and out-of-plane textures, with small full-width-half-maximum values ($\Delta\phi$ and $\Delta\omega$) in phi and omega scans. The $\Delta\phi$ and $\Delta\omega$ values were measured to be 3.7° and 1.4° , similar to those measured from the ~ 1 μm thick films.

Microstructure of SmBCO film. Figure 4 shows scanning electron microscope (SEM) and transmission electron microscope (TEM) images of the 5 μm -thick SmBCO film. The planar-view SEM image that is shown in Fig. 4(A) demonstrates that the film has a very smooth and dense surface with a few rectangular-shaped surface particles. Cross-sectional TEM images for a region including these surface particles confirm that these particles are *a*-axis oriented grains. As shown in Fig. 4(B) and (C), the particles begin to form at film thicknesses of more than 1–2 μm from the bottom of the film, grow in the shape of an upside-down quadrangular pyramid, and finally protrude out of the film. The protrusion of the particles out of the film is likely to be caused by the difference in the growth rate between the *a*-axis (or *b*-axis) and *c*-axis directions. The growth rate in the *a* or *b* direction is higher than that in the *c* direction¹⁸. Selected area diffraction (SAD) patterns, Fig. 4(D) and Fig. 4(E), obtained from the positions of 1 and 2, respectively in Fig. 4(B) confirm that the particles are *a*-axis oriented, while the matrix has *c*-axis orientation.

The volume fraction of *a*-axis-oriented grains out of the total volume of the film is estimated to be less than 1%, based on the examination of multiple TEM images, which is remarkably smaller than for those typically observed in the several-micron-thick REBCO films reported previously¹⁹.

Discussion

The degradation of structural properties, including the loss of texture and the formation of a large percentage of *a*-axis-oriented grains, results in the formation of a so-called “dead layer” above a certain critical thickness, and this is considered a major detrimental factor that will reduce J_c and thereby prevent a proportional increase of I_c with thickness^{20,21}. Unlike previous reports, in fact, no exponential decay of I_c with thickness is observed in this study for samples fabricated under optimized conditions. Similar J_c of ~ 3 MA/cm² is obtained from both ~ 1 μm thick and 5 μm thick SmBCO films grown under optimized conditions. The lack of any degradation in structural properties with thickness plays a critical role in maintaining high J_c and consequently, high I_c for these thick films.

In summary, record I_c at 77 K, self-field, exceeding 1,500 A/cm-width, was demonstrated for 5 μm -thick SmBCO film by the cost-effective, scalable EDDC process. A higher I_c exceeding 1.5 kA/cm-width is possible by further increasing the SmBCO layer thickness. This was made possible by optimization via a unique combinatorial method, which is broadly applicable for co-evaporation of other promising complex materials containing several cations. This EDDC technique and the combinatorial method that is possible using this technique, as suggested in this study, could prove invaluable in fabrication of other complex, high-performance, functional materials.

Methods

Sample preparation. SmBCO films were deposited on the IBAD-MgO templates using co-evaporation method in EDDC system. Firstly, IBAD-MgO templates were spot-welded on the drum of EDDC system, and EDDC chamber was pumped up to the total pressure of less than 5×10^{-6} Torr for more than 5 hours to provide sufficient mean free path. When the temperature of drum reached 800 °C by a heating for 2 hours, each metal source of Sm, Ba, and Cu was evaporated with a specific deposition rate, respectively. After the deposition rates were confirmed to be stable, oxygen was filled in the upper reaction chamber up to the partial pressure of 20 mTorr, and shutter was opened to start deposition toward the template surface. When deposition was finished, the EDDC chamber was filled with oxygen gas up to the pressure of 200 Torr and cooled down naturally by turning off the heater power of the drum up to room temperature. The samples were coated with silver by DC sputtering in another chamber to protect the film.

Non-contact critical current measurements. The Hall probe measurement system was used to measure the critical current distribution of SmBCO tape. The system consists of a reel to reel moving apparatus, 7 array Hall probe, a rotary encoder and a permanent magnet. The Hall probe of MULTI-7U model was fabricated in AREPOC s.r.o in Slovakia. The Hall probe consists of 7 independent Hall sensors with the interval of 600 μm , and the active area of each elementary sensor is 100 $\mu\text{m} \times$

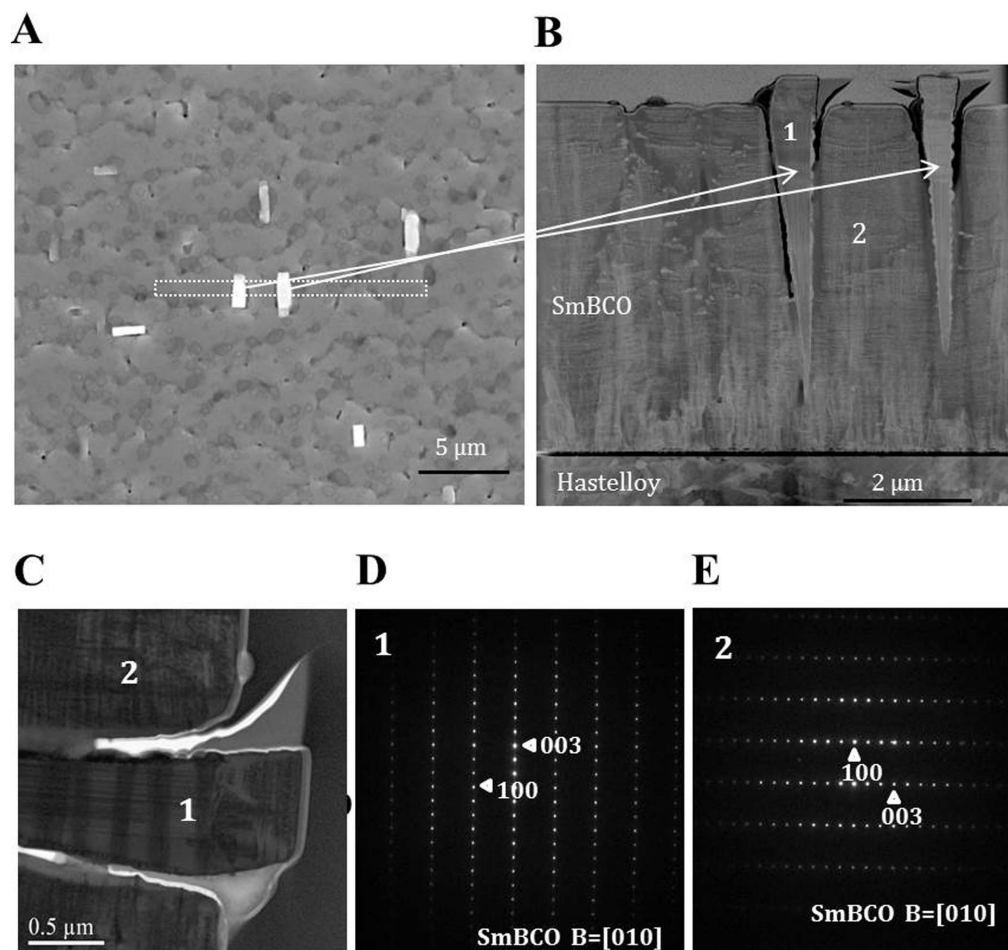


Figure 4 | SEM and TEM micrographs and electron diffraction patterns of 5 μm -thick SmBCO film. (A) SEM planar-view image of SmBCO layer, where the rectangular part of the dotted line was cut with a focused ion beam (FIB). (B) Cross-sectional scanning TEM — annular dark-field (STEM-ADF) image of rectangular area in (A), where 1 and 2 indicate an a -axis grown grain and the c -axis grown-matrix, respectively. (C) Enlarged TEM bright field (TEM-BF) image of (B), including the a -axis grown grain. (D), (E) Electron diffraction patterns of 1 and 2 in (C).

100 μm . The permanent magnet was located above Hall probe sensor, and superconducting tape passed between them. While reel to reel moving system transferred superconducting tape from feeding reel to take-up reel, the rotary encoder monitored tape position and Hall probe measured the magnetic profile across the width of superconducting tape, and computer calculated critical current from it. The critical current measured by Hall probe method was calibrated by the value of DC transport method.

Transmission Electron Microscopy (TEM) measurements. TEM specimens were fabricated in a dual beam FIB (FEI Quanta 3D FEG, Hillsboro, Oregon, USA). Target area for TEM sampling was selected using a secondary electron imaging in 20 kV and cross-sectional specimen was prepared by Ga^+ ion milling accelerated to 5–30 kV. Growth direction and phase information were investigated with the combined analyses of TEM SAD patterns and BF images using a field emission TEM (JEOL JEM-2100F, JEOL Ltd., Akishima, Tokyo, Japan) in 200 kV.

- Goyal, A. *et al.* High critical current density superconducting tapes by epitaxial deposition of $\text{YBa}_2\text{Cu}_3\text{O}_x$ thick films on biaxially textured metals. *Appl. Phys. Lett.* **69**, 1795–1797 (1996).
- Wang, C. P. *et al.* Deposition of in-plane textured MgO on amorphous Si_3N_4 substrates by ion-beam-assisted deposition and comparisons with ion-beam-assisted deposited yttria-stabilized-zirconia. *Appl. Phys. Lett.* **71**, 2955–2957 (1997).
- Macmanus-Driscoll, J. L. *et al.* Strongly Enhanced Flux Pinning in BaZrO_3 -Doped $\text{YBa}_2\text{Cu}_3\text{O}_{7-x}$ Coated Conductors. *Nature Materials*. **3**, 439–443 (2004).
- Kang, S. *et al.* High-Performance High- T_c Superconducting Wires. *Science* **311**, 1911–1914 (2006).
- Feldmann, D. M. *et al.* 1000 A cm^{-1} in a 2 μm thick $\text{YBa}_2\text{Cu}_3\text{O}_{7-x}$ film with BaZrO_3 and Y_2O_3 additions. *Supercond. Sci. Technol.* **23**, 115016–115023 (2010).
- Selvamanickam, V. *et al.* Progress in second-generation HTS wire development and manufacturing. *Physica C*. **468**, 1504–1509 (2008).
- Kutami, H. *et al.* Progress in research and development on long length coated conductors in Fujikura. *Physica C*. **469**, 1290–1293 (2009).
- MacManus-Driscoll, J. L. & Wimbush, S. C. Future directions for cuprate conductors. *IEEE Trans. Appl. Supercond.* **21**, 2495–2500 (2011).
- Dürschmabel, M. *et al.* $\text{DyBa}_2\text{Cu}_3\text{O}_{7-x}$ superconducting coated conductors with critical currents exceeding 1000 A cm^{-1} . *Supercond. Sci. Technol.* **25**, 105007–105011 (2012).
- Foltyn, S. R. *et al.* Materials science challenges for high-temperature superconducting wire. *Nature Materials* **6**, 631–642 (2007).
- Foltyn, S. R. *et al.* Relationship between film thickness and the critical current of $\text{YBa}_2\text{Cu}_3\text{O}_{7-x}$ coated conductors. *Appl. Phys. Lett.* **75**, 3692–3694 (1999).
- Lee, B. S. *et al.* Fabrication of $\text{Sm}_1\text{Ba}_2\text{Cu}_3\text{O}_7$ coated conductors using the co-evaporation method. *Supercond. Sci. Technol.* **17**, 580–584 (2004).
- Kim, H. S. *et al.* Effect of the composition on the superconducting properties of IBAD-MgO SmBCO coated conductors with superconducting film directly deposited on epi-MgO layer. *Physica C*. **471**, 932–936 (2011).
- Oh, S. S. *et al.* Development of long-length SmBCO coated conductors using a batch-type reactive co-evaporation method. *Supercond. Sci. Technol.* **21**, 34003–34008 (2008).
- Hayashi, T. *et al.* Effect of composition gradient in Cu(In,Al)Se_2 solar cells. *Solar Energy Materials and Solar Cells*. **93**, 922–925 (2009).
- Ikeda, T. *et al.* A combinatorial approach to microstructure and thermopower of bulk thermoelectric materials: the pseudo-ternary $\text{PbTe-Ag}_2\text{Te-Sb}_2\text{Te}_3$ system. *J. Materials Chemistry*. **22**, 24335–24347 (2012).
- Kim, H. S. *et al.* Nondestructive Measurement of Critical Current Distribution of SmBCO Coated Conductor using Hall Probe. *IEEE Trans. Appl. Supercond.* **20**, 1537–1540 (2010).
- Muller, D. & Freyhardt, H. C. Growth model for melt-textured $\text{Y}_1\text{Ba}_2\text{Cu}_3\text{O}_{7-x}$. *Physica C*. **242**, 283–290 (1995).
- Ibi, A. *et al.* Investigations of thick YBCO coated conductor with high critical current using IBAD-PLD method. *Physica C*. **426–431**, 910–914 (2005).



20. Leonard, K. *et al.* Thickness dependence of microstructure and critical current density of $\text{YBa}_2\text{Cu}_3\text{O}_{7-\delta}$ on rolling-assisted biaxially textured substrates. *J. Mater. Res.* **18**, 1109–1122 (2003).
21. Takahashi, Y. *et al.* Thickness dependence of I_c and J_c of LTG-SmBCO coated-conductor on IBAD-MgO tapes. *Physica C.* **471**, 937–939 (2011).

Acknowledgments

This research was supported by a grant from Center for Applied Superconductivity Technology of the 21st Century Frontier R&D Program funded by the Ministry of Science and Technology in Korea. The authors wish to thank Mr. S.H. Jang and Mr. C.H. Min for their help in the fabrication of samples and Mr. Lawrence Cho for his contribution to sample preparation for TEM. Work at Oak Ridge National Laboratory was sponsored by the U.S. DOE Office of Electricity Delivery and Energy Reliability - Advanced Cables and Conductors under contract DE-AC05-00OR22725 with UT-Battelle, LLC managing contractor for Oak Ridge National Laboratory.

Author contributions

H.S.K. designed the research and conducted all the experiments. H.S.K. and S.S.O. analyzed the data and wrote the manuscript. H.S.H. contributed to the measurement of critical

current property of the samples. D.Y. contributed the design of experimental apparatus. S.H.M. fabricated buffered substrates. J.H.K. and Y.U.H. conducted TEM analysis of the samples. S.X.D. has been collaborating with J.H.K. and joined the discussion for this study. S.H.W. conducted XRD analysis of the samples. A.G. contributed to the discussion and edited the manuscript. All authors reviewed the manuscript.

Additional information

Supplementary information accompanies this paper at <http://www.nature.com/scientificreports>

Competing financial interests: The authors declare no competing financial interests.

How to cite this article: Kim, H.-S. *et al.* Ultra-High Performance, High-Temperature Superconducting Wires via Cost-effective, Scalable, Co-evaporation Process. *Sci. Rep.* **4**, 4744; DOI:10.1038/srep04744 (2014).



This work is licensed under a Creative Commons Attribution-NonCommercial-NoDerivs 3.0 Unported License. The images in this article are included in the article's Creative Commons license, unless indicated otherwise in the image credit; if the image is not included under the Creative Commons license, users will need to obtain permission from the license holder in order to reproduce the image. To view a copy of this license, visit <http://creativecommons.org/licenses/by-nc-nd/3.0/>